Supplementary information

Table S1 Fundamental properties of raw materials and amendments

Material	Main component	Mass fraction%	pH	EC/(μS·cm^{-1})	ρ_b/(g·cm^{-3})	ρ_p/(g·cm^{-3})	f_0/%	Particle size/μm
Opal	$SiO_2 \cdot nH_2O$ (amorphous)	98.11	7.65±0.01	55.90±0.40	0.51±0.01	2.22±0.01	76.83±0.08	75−50
Sand	SiO_2 (Quartz)	80.25	9.22±0.03	94.47±0.21	1.24±0.01	2.66±0.03	53.29±0.19	~75
Limestone	$CaCO_3$	>96	8.32±0.03	65.47±0.42	—	—	—	75−50
Desulfuration gypsum	$CaSO_4 \cdot 2H_2O$	>98	7.46±0.10	940.67±3.06	—	—	—	
Tricalcium phosphate	$Ca_3(PO_4)_2$	>99	12.28±0.03	1934.00±1.00	—	—	—	
Hematite	Fe_2O_3	>95	6.47±0.01	157.57±1.31	—	—	—	
Gibbsites	$Al(OH)_3$	>68	9.96±0.01	128.43±0.35	—	—	—	

Note: EC−Electrical conductivity; ρ_b−Bulk density; ρ_p−Particle density; f_0−Porosity; Mean±SD (n=3).

Table S2 Bulk density (ρ_b), particle density (ρ_p), and porosity (f_0) of aggregates

Parameter	Dosage of inorganic minerals/wt.%	OSC	OSG	OSP	OSA	Dosage of Fe_2O_3/wt.%	OSI
Bulk density (ρ_b)	0	0.67±0.02a	0.67±0.02a	0.67±0.02a	0.67±0.02a	0	0.67±0.02a
	2	0.57±0.02 b	0.56±0.01c	0.62±0.03ab	0.63±0.02b	1	0.59±0.01c
	5	0.6±0.02b	0.59±0.02bc	0.62±0.03ab	0.63±0.01b	2	0.6±0.01c
	8	0.61±0.03b	0.64±0.02a	0.61±0.02bc	0.62±0.02b	4	0.61±0.01c
	10	0.62±0.02b	0.63±0.05ab	0.56±0.01c	0.61±0.02b	5	0.64±0.01b
Particle density (ρ_p)	0	2.48±0.03a	2.48±0.03a	2.48±0.03a	2.48±0.03c	0	2.48±0.03c
	2	2.47±0.05a	2.39±0.02bc	2.48±0.06a	2.57±0.06ab	1	2.48±0.04c
	5	2.35±0.01c	2.34±0.02c	2.43±0.05a	2.58±0.08ab	2	2.61±0.00a
	8	2.39±0.01bc	2.39±0.04bc	2.41±0.06a	2.60±0.04a	4	2.63±0.03a
	10	2.43±0.01ab	2.43±0.05ab	2.49±0.05a	2.55±0.06ab	5	2.56±0.04b
Porosity (f_0)	0	72.78±0.03c	72.78±0.03b	72.78±0.03c	72.78±0.03b	0	72.78±0.03c
	2	76.90±0.51a	76.75±0.23a	74.94±0.64b	75.65±0.58a	1	76.07±0.38ab
	5	74.59±0.09b	74.13±1.55b	74.40±0.55b	75.72±0.78a	2	77.15±0.02a
	8	74.40±0.04b	73.55±0.33b	74.65±0.64b	76.20±0.37a	4	76.75±0.25ab
	10	74.55±0.05b	74.10±0.51b	77.52±0.45a	75.98±0.54a	5	75.05±0.38b

Note: Mean±SD (n=3). Different letters indicated significant differences among different treatments in each inorganic mineral.

Table S3 Atomic orbital binding energy (BE) and atomic number fraction of elements in aggregates before and after inorganic mineral treatment

Aggregate	O 1s		Si 2p		Amendments		
	BE	Mass fraction/wt.%	BE	Mass fraction/wt.%		BE	Mass fraction/wt.%
CK	532.42	55.02	103.13	24.78		—	—
OSC	532.6	62.25	103.29	27.35		347.24	0.77
OSG	532.47	62.54	103.19	25.88	Ca 2p	347.77	1.18
OSP	532.48	58.54	103.24	22.6		347.31	5.25
OSI	532.69	60.25	103.35	25.23	Fe 2p	710.71	2.16
OSA	532.41	60.41	103.31	19.44	Al 2p	74.17	6.91

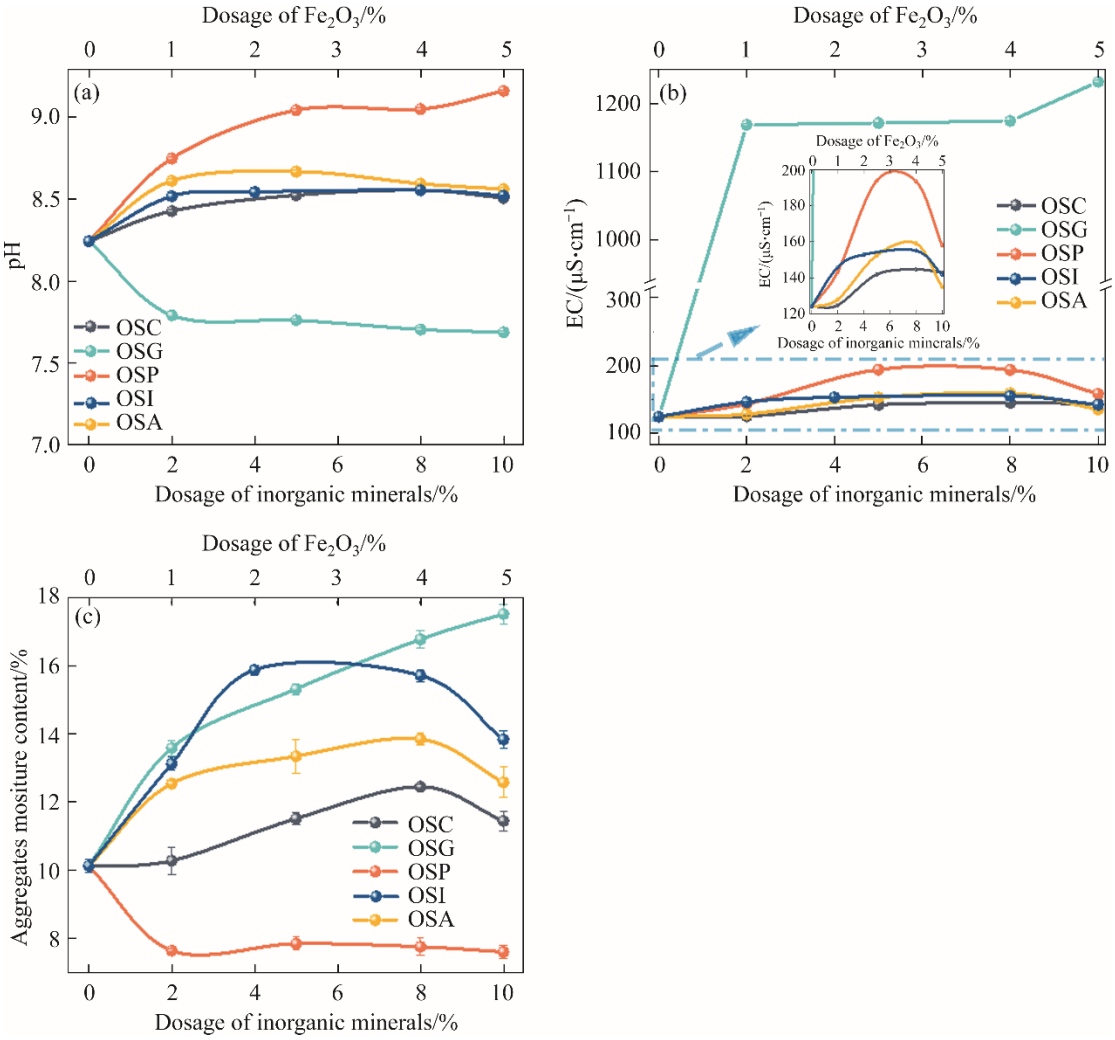

Figure S1 Physico-chemical properties of aggregates after different treatments: (a) pH; (b) EC; (c) WC (The top horizontal coordinate in the figure corresponds to the OSI aggregate, while bottom horizontal coordinate corresponds to the other aggregates)

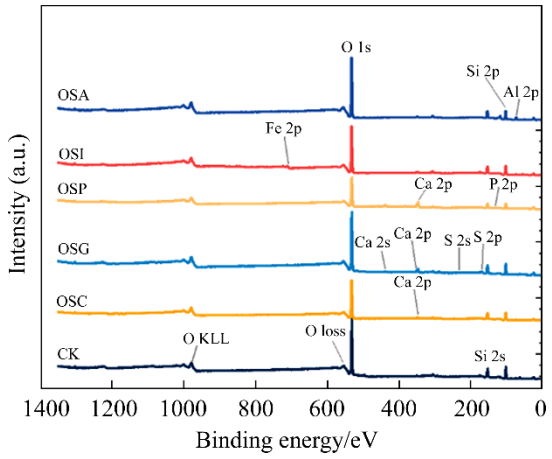

Figure S2 XPS full spectrum of aggregates before and after amendments treatment

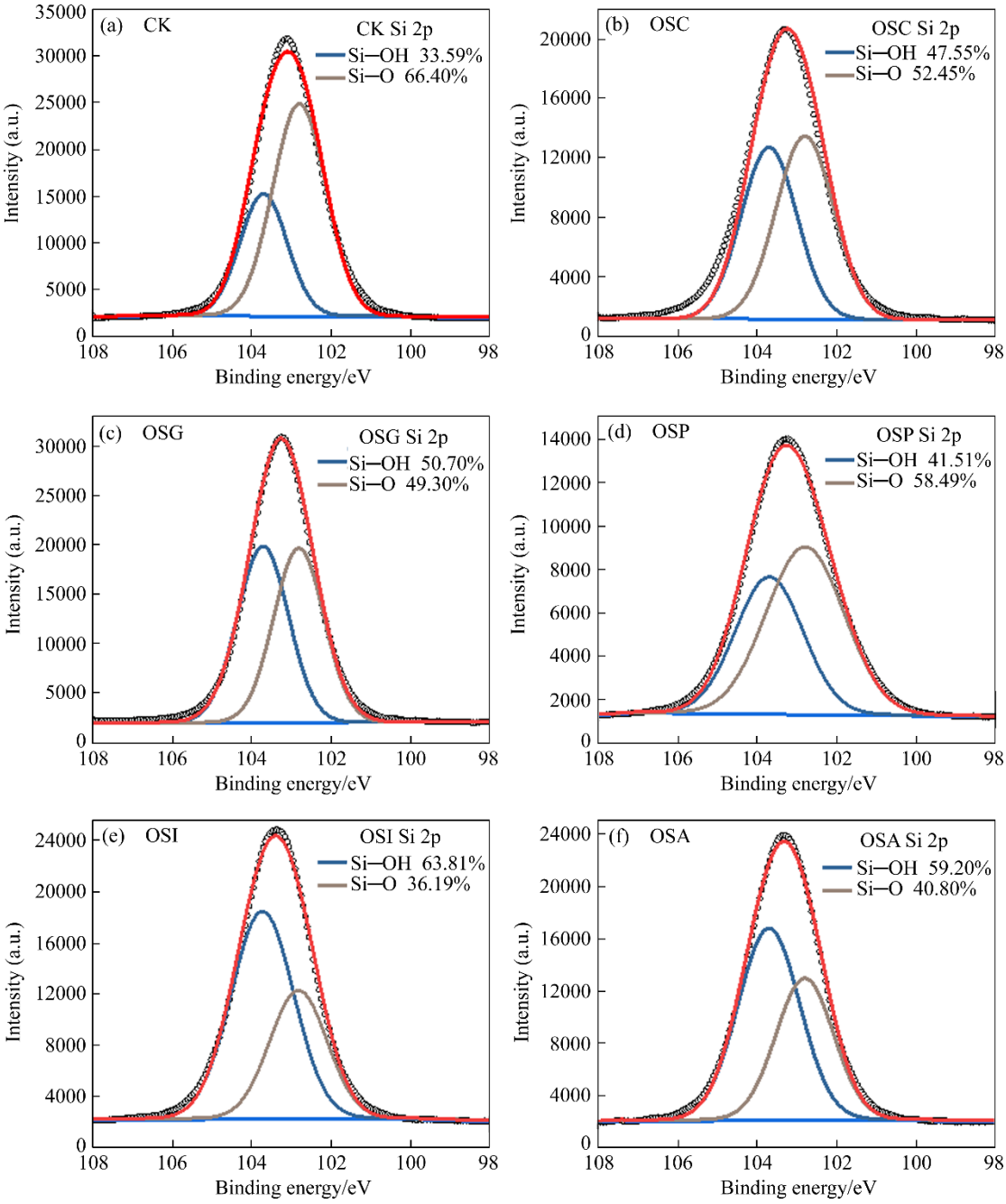

Figure S3 Si 2p XPS high-resolution spectrum of aggregates before and after amendments treatment

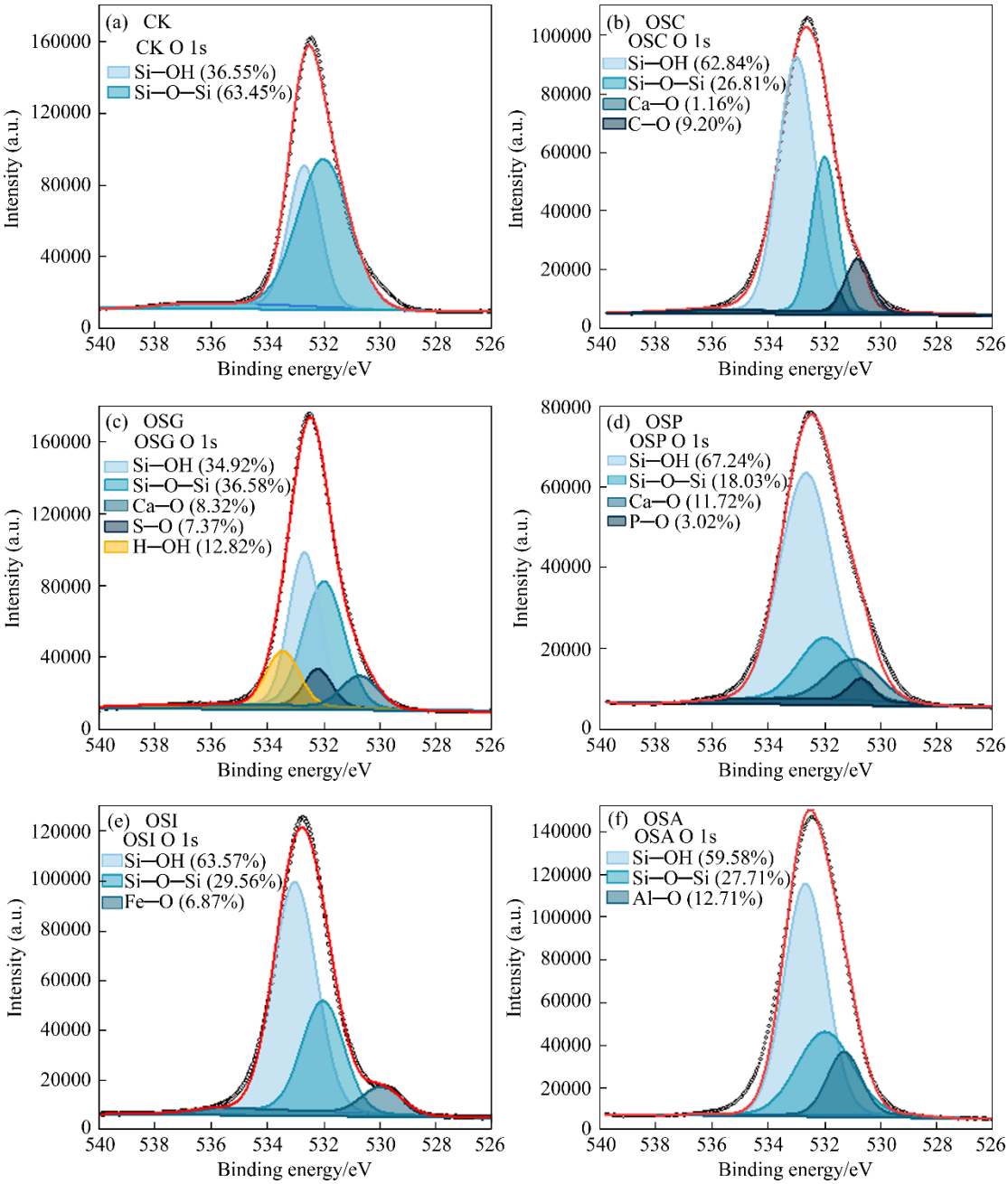

Figure S4 O 1s XPS high-resolution spectrum of aggregates before and after amendments treatment

Figures S3 and S4 showed the XPS high-resolution fitted spectra of Si 2p and O 1s of the aggregates before and after amendment, respectively. Si 2p and O 1s in CK originated from opal (Si—OH/Si—O) and quartz in the sand (Si—O), exhibiting a single and symmetrical peak pattern. The fitted integrated area reflects the relative content of this group. The content of Si—OH increased after the amendment; particularly, the application of Ca-containing minerals (Figure S3(b)−(d)), with OSG displaying the highest increase at 50.70%; following Fe_2O_3 and $Al(OH)_3$ treatment (Figures S3(e)−(f)), the Si—OH content further increased. The O 1s symmetry decreased upon the addition of Ca-containing minerals (Figures S4(b)−(d)), accompanied by the appearance of Me—O (Ca—O/Fe—O/Al—O) and C—O/S—O/P—O groups, whereas the Si—O content decreased. The O 1s peak symmetry dropped even further following Fe_2O_3 and $Al(OH)_3$ treatment (Figures S4(e)−(f)), wherein Fe—O (529.9 eV) and Al—O (531.3 eV) emerged in addition to Si—OH and Si—O, respectively. This was because

more Si-OH formed on the aggregate surface in the presence of amendments and water; the metal ions (Ca^{2+}/Fe^{3+}/Al^{3+}) in the amendments chemisorbed with O on the surface of sand and opal, altering the shape and symmetry of O 1s, and generating Me—O—Si bonds; the O on the hydroxyl complexes diluted the Si—O content, indirectly reducing the Si—O content. These findings further confirmed the Si—OH on the surface of the opal adsorbed with the —Si—O—Si— on the surface of sand particles in the presence of water and amendments, favoring aggregate formation. However, the formation of unstable cyclic Si—O groups cannot be excluded.

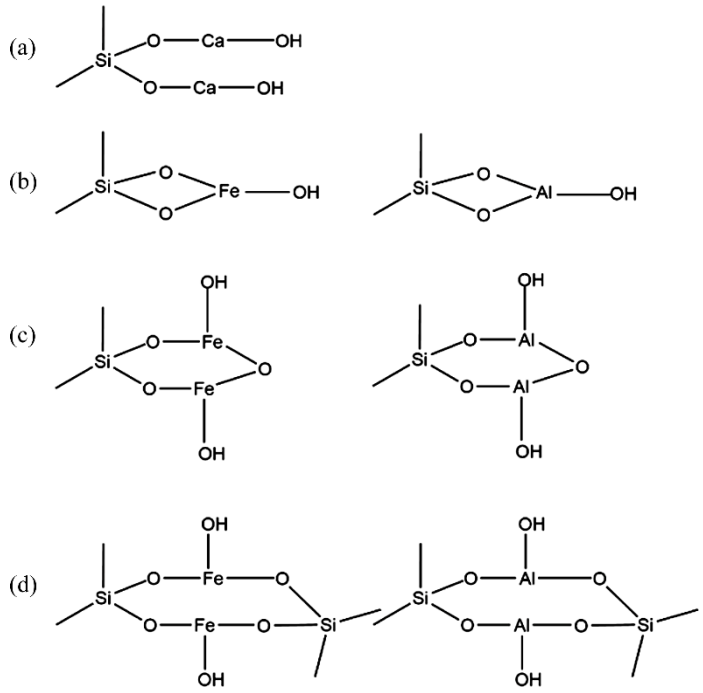

Figure S5 Possible chemical structures of amendments adsorbed to opal/sand